Extraction of Soil Moisture Value Using ALOS PALSAR Data

Rahmawati Putri and Pakhrur Razi

Abstract Soil moisture is an essential factor in determining the dryness level of an area. Generally, soil moisture is carried out manually, which takes a long time and is expensive. However, we extracted soil moisture values using SAR satellite data in this research. SAR satellite data has the advantage that it can be used during the day and night and in various weather conditions. This research extracted soil moisture values with ALOS PALSAR data and SNAP processing. Based on this research, most of Padang has high soil moisture levels. On a map of 11 sub-districts, 4 are high-humidity sub-districts, and 7 are sub-districts with moderate soil moisture levels, for sub-districts with high humidity levels, namely Kuranji District, Nanggalo District, North Padang District, and East Padang District.

Keywords Soil moisture · Alos Palsar · SAR · SNAP · Padang

1 Introduction

The city of Padang has an area of 1,414.96 km^2 with a land area of 694.96 km^2 The city of Padang has an area of 1,414.96 km^2 with a land area of 694.96 km^2 [1] and an ocean area of 720.00 km^2 [2]. The city has a relatively sloping topography and is not steep in a densely populated area. The area of Padang City, located on the west coast of Sumatra Island, has a topography of lowlands, hills, and watersheds [3]. The city of Padang was likely to have an earthquake because it was triggered by the Semangko Fault and tectonic activity in the subduction zone [4, 5]. In addition, most of the coastal area of Padang City is a swamp area with many buildings on it. If an

R. Putri · P. Razi (✉)
Department of Physics, Faculty of Mathematics and Natural Sciences, Universitas Negeri Padang, Jl. Prof Hamka, Padang 25131, Indonesia
e-mail: fhrrazi@fmipa.unp.ac.id

Research Center of Disaster Monitoring and Earth Observation, Universitas Negeri Padang, West Sumatra, Padang 25131, Indonesia

J. T. Sri Sumantyo and P. Razi (eds.), *Advances in Geoscience and Remote Sensing Technology*, Springer Proceedings in Earth and Environmental Sciences,
https://doi.org/10.1007/978-981-97-5746-6_27

earthquake occurs, it will be dangerous for buildings and residents in the area. One of the problems caused by the earthquake is the danger of liquefaction [6].

Earthquakes are one of the factors that may cause liquefaction. Liquefaction occurs because the soil loses weight in a short time [7–9]. This event causes a change in the soil structure from solid to liquid [10–12]. One of the indicators to determine the liquefaction susceptibility zone is soil moisture. Soil moisture is the amount of water stored in the soil pores [13, 14]. The value of soil moisture can be seen by observing the radar image [15–17]. Radar has a function to detect objects that are very far away, detect the speed of the object being observed, and detect satellites or outer space orbits [18, 19]. Radar images were observed using the SAR method [20]. SAR is a coherent radar system that forms high-resolution remote sensing imagery [21, 22] that can be used day and night in all weather conditions [23–27]. This is because the SAR system uses radio waves (microwaves) to observe the earth's surface. The SAR system consists of a transmitter, antenna, sensor receiver, and an electronic system used to record data. Mapping performed using SAR is a fairly effective method that can cover a large area [28] in a short time estimate [5], has low cost [29], and has very high credibility in the implementation, especially for disaster monitoring [30, 31]. The SAR work system, among others, sends pulses and microwave energy to the desired object by recording the reflected strength received by the object in the imaging area [32].

2 Study Area and Satellite Dataset

2.1 Study Area

The research location is in Padang City, which has an area of 1,414.96 km^2 with a land area of 694.96 km^2 and a sea area of 720.00 km^2. This city has a relatively gentle and not steep topography and is a densely populated area. The locations of this research are in the East Padang District, North Padang District, Nanggalo District, and Kuranji District (Fig. 1).

2.2 Satellite Dataset

This research uses data from Alos Palsar imagery. PALSAR is one of three instruments on the Advanced Land Observing Satellite (ALOS), also known as DAICHI, developed to contribute to mapping, precise regional land cover observation, disaster monitoring, and resource surveying. ALOS is a mission of the Japan Aerospace Exploration Agency (JAXA).

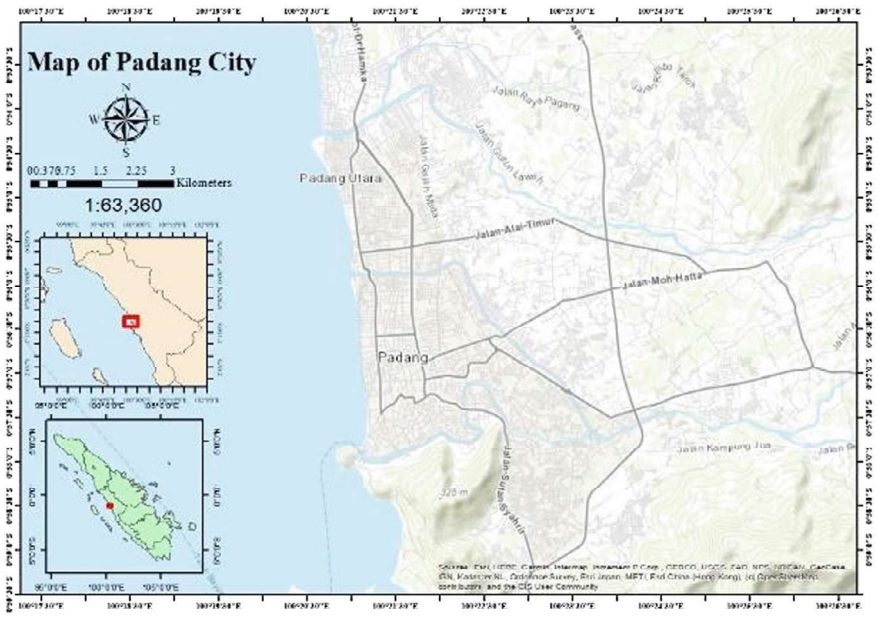

Fig. 1 Research map

3 Methods

This research is applied research to solve a problem that focuses on its application in everyday life. This research measures the value of soil moisture as an indicator of the liquefaction vulnerability zone, which is expected to provide practical solutions to problems and can be a solution in dealing with potential liquefaction hazards. This research was conducted in three stages: preparation, data collection, and report preparation. Then, data collection includes image data processing to remove the atmospheric disturbance using filtering and multi-looking [33] and downloading the required software. Then, data collection includes image data processing and retrieval of measurement data in the field. The last stage is the preparation of reports and research results that will be in seminars. The variables used in this study are time on the satellite used, Soil Moisture, and the area of Padang City. The stages of the research can be described in detail as follows (Fig. 2).

The preparation stage is in the form of a literature study and preparation of the equipment used in the research. This literature study was conducted to improve the researcher's understanding of relevant theories on the liquefaction problem. Data was collected to obtain the information needed to achieve the research objectives. The authors collected data from the ALOS PALSAR 1.1 satellite imagery in this study. This stage includes data calibration, multi-looking, speckle filtering, ALOS deskewing, and terrain correction. The goal is that the processed image has been calibrated beforehand, reduces speckles, and the image can look like the original.

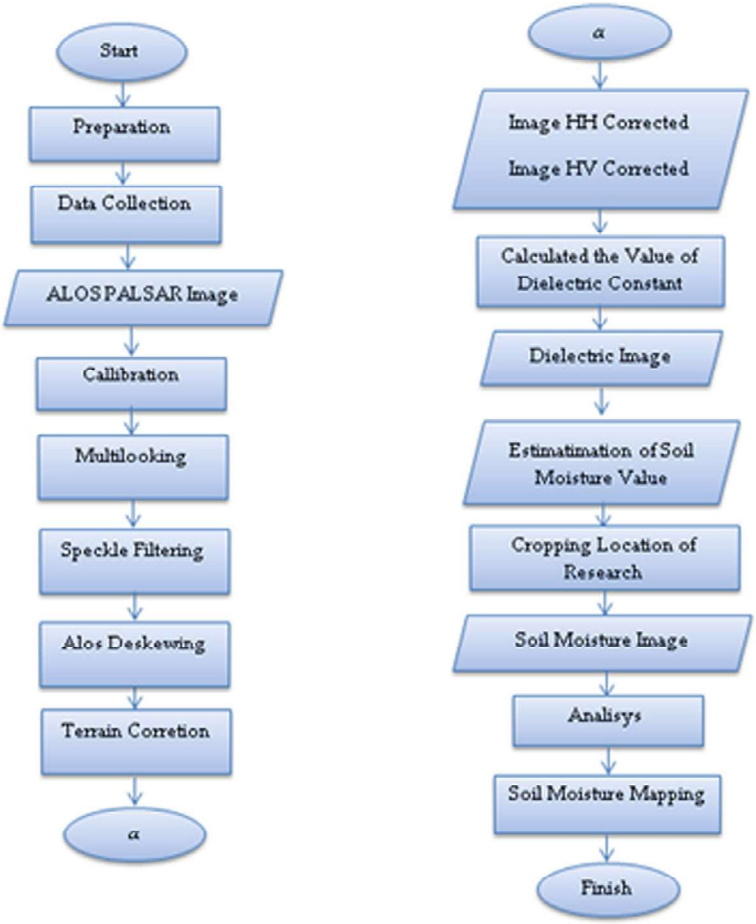

Fig. 2 Research stage

Calculating the dielectric constant is necessary because the value of the dielectric constant affects the results of the estimated soil moisture value. To estimate the value of soil moisture, it is necessary to convert the digital values of ALOS PALSAR polarization (HH and HV) into backscatter values using Eq. 1 [34].

$$\sigma^0 = 10 \log_{10} DN^2 + CF \tag{1}$$

Description:

σ^0: Backscatter coefficient (dB).
DN: Average digital image value.
CF: Calibration factor (standard deviation 0.64 dB used).

Based on the backscattering coefficient, an estimation of the value of the dielectric constant is made using Eq. 2.

$$\acute{\epsilon} = \frac{\log_{10}\left(\frac{(\sigma^0_{HH})^{0.7857}}{(\sigma^0_{HV}}\right) 10^{-0.19} \cos^{1.82}\theta \sin^{0.93}\theta \lambda^{0.15}}{-0.024 \tan\theta} \quad (2)$$

Description:

ɛ́: Dielectric constant.
σ^0: Sigma Nought (dB).

After estimating the dielectric constant value, calculate the surface roughness value using Eq. 3.

$$ks = \sigma_{HH}^{o\frac{1}{1.4}} 10^{\frac{2.75}{1.4}} \frac{\sin^{2.57}\theta}{\cos^{1.07}\theta} 10^{-0.02\varepsilon \cdot \tan\theta} \lambda^{-0.5} \quad (3)$$

Description:

Ks: Surface roughness.
ɛ́: Dielectric constant.
σ^0: Backscatter coefficient.
θ: Angle formed (°).
λ: Wavelength (23.6 cm).

To determine the value of soil moisture, it is necessary to estimate the value of soil moisture calculated in Eq. 4 [35].

$$M_v = \left(-5.3 \times 10^{-2} + 2.29 \times 10^{-2}\acute{\epsilon} - 5.5 \times 10^{-4}\acute{\epsilon}^2 + 4.3 \times 10^{-6}\acute{\epsilon}^3\right) \quad (4)$$

Description:

M_v: Soil moisture (%).
ɛ́: Dielectric constant.

After obtaining the dielectric constant value and surface roughness, it is possible to calculate the soil moisture value using Eq. (4). Cropping is done to crop the image according to the boundaries of the research location, namely the Padang City area. At this stage, the difference in soil moisture values is analyzed in the estimation results of soil moisture values with ALOS-PALSAR satellite image data and data from measurements in the field. A soil moisture map containing soil moisture values in Padang was created using ArcGIS 10.3 software. Data collection techniques in this study use SAR (Synthetic Aperture Radar). The collected data is then processed using SNAP (Sentinel Application Platform). This SAR data is in the form of satellite imagery. The satellite image is processed using the soil moisture formula to produce a soil moisture image. After that, the soil moisture image is obtained and made into a soil moisture map using ArcGIS. The data collected is in the form of ALOS

PALSAR images. This image was processed to get the soil moisture value in the city of Padang. soil moisture image is used as an indicator to see the liquefaction vulnerability zone. The processed images are then grouped based on the sub-districts in the city of Padang. It aims to see and analyze the sub-districts in Padang City in more detail and determine which areas have low, medium, and high soil moisture and liquefaction potential.

4 Results and Discussion

This research uses images from the ALOS PALSAR satellite. This study aimed to produce a soil moisture map in the city of Padang. From the results of this study, information was obtained in the form of estimated soil moisture values in various sub-districts in Padang City so that it could be an indicator to determine the liquefaction vulnerability zone.

The dielectric constant is needed in image processing using the soil moisture formula. Terrain correction results for HH and HV can be seen in Fig. 3a and b.

The process of processing soil moisture values begins with finding the backscattering coefficient (dB). The backscatter coefficient value is searched using Eq. 1. The results of the processing of the HH and HV backscatter values are shown in Fig. 4a and b.

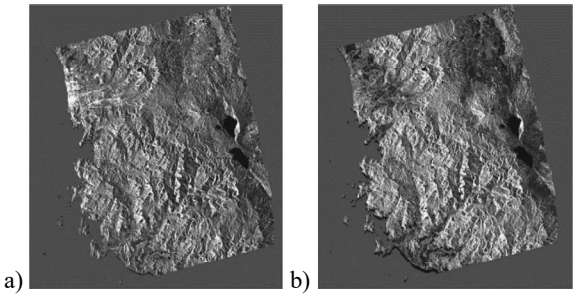

Fig. 3 The result of the terrain correction process: **a** the results of the terrain correction process for HH; **b** the results of the terrain correction process for HV

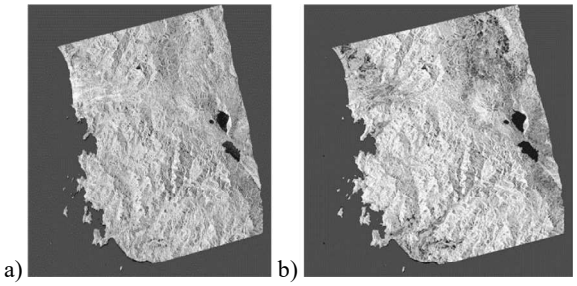

Fig. 4 The result of the backscattering coefficient: **a** the result of the backscattering coefficient for HH; **b** the result of the backscattering coefficient for HV

Furthermore, data processing is carried out to obtain an estimate of the value of the dielectric constant using Eq. 2 (Fig. 5).

The next step is to calculate the surface roughness value using Eq. 3. The results of processing the surface roughness value can be seen in Fig. 6.

After getting the backscattering coefficient, dielectric constant, and ground surface roughness, the next step is to estimate the soil moisture value using Eq. 4. The results of the estimated soil moisture value can be seen in Fig. 7.

Soil moisture values are grouped based on the soil moisture value and the color range shown in maps. From the maps, it can be seen that the soil moisture in yellow

Fig. 5 Processing results to calculate the value of the dielectric constant

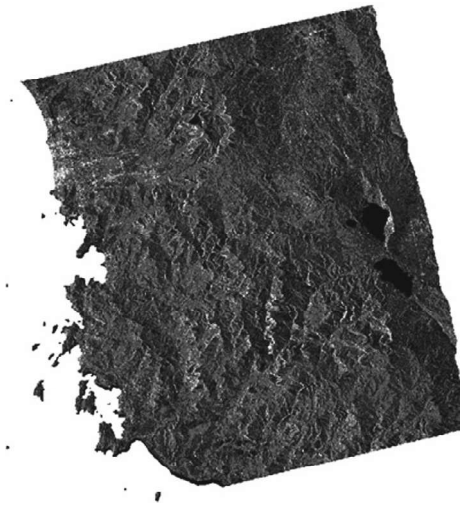

Fig. 6 Result of processing to calculate the surface roughness

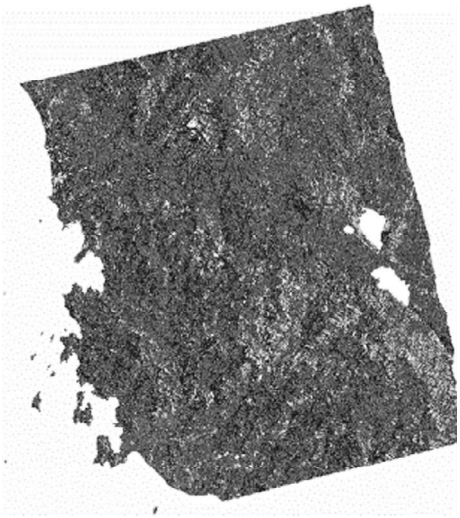

Fig. 7 Results of processing to estimate the value of soil moisture

has a shallow level of soil moisture. The green color has a low level of soil moisture. Soil moisture in dark green has moderate soil moisture, light blue has high soil moisture, and dark blue has a very high soil moisture level. The soil moisture level's color is determined from the ALOS PALSAR data. After obtaining the soil moisture level, the image is cut based on the research location, namely the city of Padang. The images are cropped per sub-district in Padang City and shown in Figs. 8, 9, 10, and 11.

1. East Padang

East Padang District is one of the districts in Padang City. Administratively, this sub-district has an area of 8.15 km^2. The soil moisture value map for East Padang District is shown in Fig. 8. The study's results found that light blue and dark blue colors dominated soil moisture in East Padang District. This indicates that the area has a high soil moisture value, such as in the Ganting Parak Gadang area, Kubu Dalam Parak Karakah, some areas of Jati, and East Sawahan. A small part of the Jati and Sawahan Timur areas looks dark green, which means the area has a moderate soil moisture value. However, dark blue and light blue colors dominate this area, and it can be concluded that Padang Timur District has soil moisture values with high humidity levels.

2. North Padang

North Padang District is one of the districts in Padang City. Administratively, this sub-district has an area of 8.08 km^2. The soil moisture value map for Padang Timur District is shown in Fig. 9. Based on Fig. 9, it is found that soil moisture in North Padang District has a fairly varied color range but is dominated by light blue and dark blue, which indicates the area has a high soil moisture value, but it is also seen that in some areas there is a dark green color, which means the area has a high level of soil

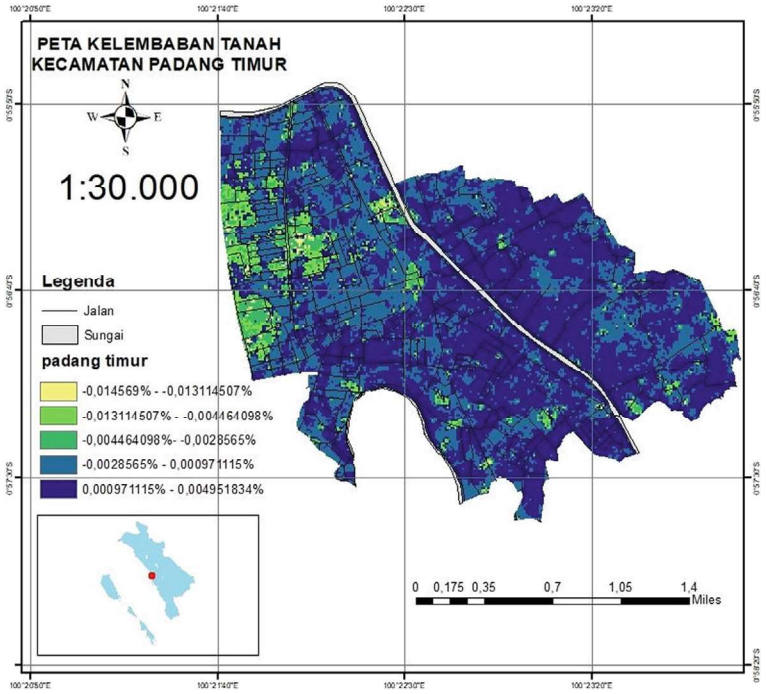

Fig. 8 Soil moisture map in East Padang district

moisture. These sites, such as the Great Mosque of West Sumatra and the vicinity of Gajah Beach, have moderate soil moisture values. The Gajah Beach area should have high soil moisture because it is close to the beach, but it can be seen on the map that this area has a moderate value. This is influenced by the number of houses and settlements in the vicinity, so that the surrounding soil moisture is lower than in other areas. Light blue and dark blue colors surround UNP, Ulak Karang, and Tabing, meaning this area has a high soil moisture value. As we know, the previous UNP area was a swamp, which makes the soil moisture in this area look high. Therefore, it can be concluded that the of North Padang, which has soil moisture values with high humidity levels.

3. Nanggalo

The district is one of the districts in Padang City. Administratively, this sub-district has an area of 8.07 km^2. The soil moisture value map for Nanggalo District is shown in Fig. 10.

According to Fig. 10, the Kurao Pagang, Siteba, and Laweh Deserts in Nanggalo District have a dominant light blue and dark blue color range, indicating that the area has a high soil moisture value. However, it is also seen in some areas that there is a green color. This means the area has moderate soil moisture values, such as

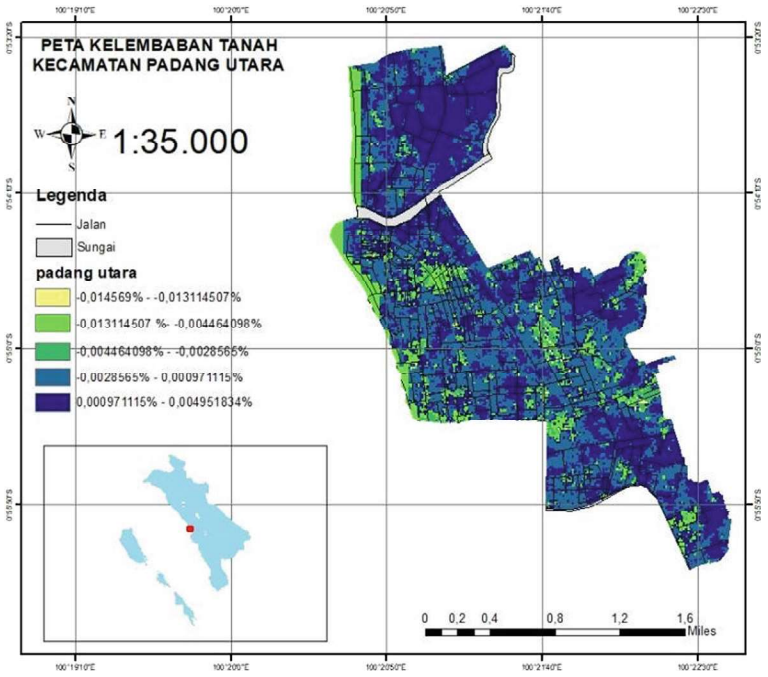

Fig. 9 Soil moisture map in North Padang district

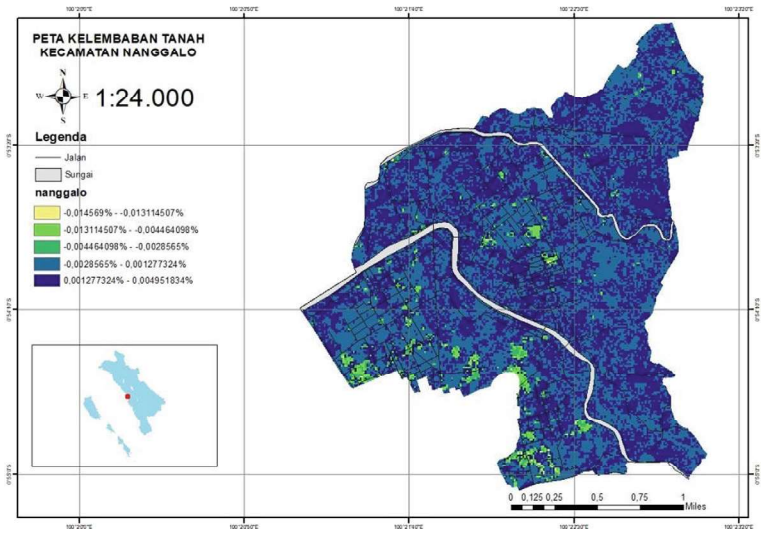

Fig. 10 Soil moisture map in Nanggalo district

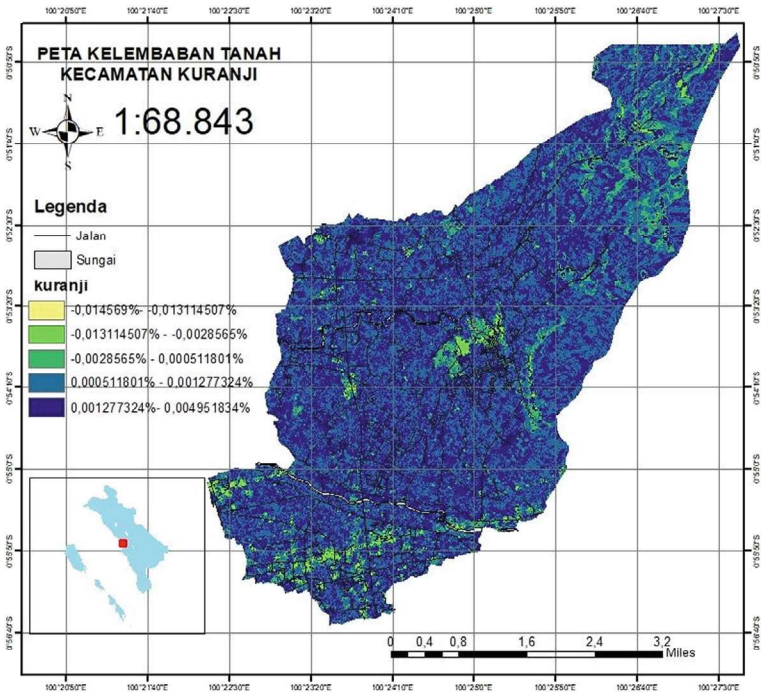

Fig. 11 Soil moisture map in Kuranji district

in Kampung Lapai and Tabing Banda Gadang. Therefore, it can be concluded that Nanggalo Subdistrict has a soil moisture value with a high humidity level.

4. Kuranji

Kuranji District is one of the districts in Padang City. Administratively, this subdistrict has an area of 54.41 km^2. The soil moisture value map for Kuranji District is shown in Fig. 11.

According to Fig. 11, the soil moisture in Kuranji District has a light blue and dark blue color range that indicates the area has a high soil moisture value. However, it is also seen that there is a dark green color in some areas, which means the area has a soil moisture value, which is the Anduriang area and the Starfruit Market. Meanwhile, other areas are colored light blue and dark blue, which indicates that this area has high soil moisture, such as Ampang, Sungai Sapih, and Kalumbuk. Therefore, it can be concluded that Kuranji District has soil moisture values with high humidity levels.

Based on the research results, we obtained soil moisture values in the form of tables and maps. This data is obtained by processing the ALOS PALSAR image using SNAP. This ALOS PALSAR image is then calibrated, and some pre-processing is performed. After pre-processing, the backscattering coefficients (HH and HV) value will be searched using Eq. 1. After obtaining the backscattering coefficient value,

the next step is to find the dielectric constant value using Eq. 2. Then, determine the surface roughness value using Eq. 3. After the process is carried out, The next step is to estimate the soil moisture value using Eq. 4. After the process is completed, the soil moisture value is obtained in the ALOS PALSAR image.

The resulting soil moisture image from ALOS PALSAR is then processed and converted into a map using ArcGIS. The results of the ALOS PALSAR image are cut based on the research area, namely the City of Padang. After being cut based on the research area, then colored. This is intended to facilitate the distribution of soil moisture levels. The colors given are yellow with very low soil moisture levels, green with low soil moisture levels, dark green with moderate soil moisture levels, light blue with high humidity levels, and dark blue with very high soil moisture levels. After grouping the soil moisture level, the next step is to make a map based on the districts in Padang City, which are 11 districts.

These soil moisture value results are used as an indicator to determine the liquefaction vulnerability zone in Padang City. The higher the value of soil moisture, the higher the potential for liquefaction susceptibility zones because liquefaction occurs more easily in soils with a liquid structure. There are a number of factors that affect liquefaction potential, including soil moisture and soil structure [36]. If the soil moisture is high, the soil in that area has no stiffness and is easier to shift if there is a sudden vibration. Based on the results obtained on the map, the area in yellow has a very low level of soil moisture and liquefaction potential. Areas in green have low soil moisture levels and liquefaction potential. Areas in dark green have moderate levels of soil moisture and liquefaction potential. Areas in light blue have a high level of soil moisture and liquefaction potential, and areas in dark blue have a very high level of soil moisture and liquefaction potential. Therefore, from the soil moisture map, it was found that most of Padang City has a fairly high liquefaction potential because it is based on maps of 11 sub-districts, four sub-districts with high humidity levels, and seven sub-districts with moderate soil moisture levels, namely Kuranji District. Nanggalo District, North Padang District, and East Padang District.

5 Conclusions

Based on the research, it can be concluded that the city of Padang has a high soil moisture and liquefaction potential. This can be seen on the soil moisture map that has been made. The map shows four sub-districts in Padang City with high soil moisture values: Kuranji District, Nanggalo District, East Padang District, and North Padang District. Therefore, these four sub-districts have a reasonably high liquefaction potential compared to other sub-districts. Meanwhile, seven other sub-districts have moderate soil moisture values, namely Koto Tangah District, Pauh District, West Padang District, South Padang District, Lubuk Begalung District, Lubuk Kilangan District and Bungus Teluk Kabung District.

Acknowledgements The author would like to thank The United States Geological Survey (USGS), Japan Aerospace Exploration Agency (JAXA), European Space Agency for SNAP software application and BNPB.

Author Contributions Consentualization, P.R; Methodology, R.P; Validation, P.R; Resource R.P, P.R; Data Curation, R.P., PR; Draft preparation R.P, P.R

Abbreviations

SAR	Synthetic Aperture Radar
ALOS PALSAR	Advanced Land Observing Satellite Phased Array type L-Band
SNAP	Sentinel Application Platform
JAXA	Japan Aerospace Exploration Agency

References

1. G. Ananda, T. Ophiyandri, and A. Hakam, Hotels contingency assessment in Padang city against coastal hazard, *MATEC Web Conf.*, vol. 229, pp. 1–5, 2018, https://doi.org/10.1051/matecconf/201822902015.
2. F. Ashar, D. Amaratunga, P. Sridarran, and R. Haigh, *Practices of tsunami evacuation planning in Padang, Indonesia.* Elsevier Inc., 2018. https://doi.org/10.1016/B978-0-12-810473-6.00019-4.
3. H. Cressendo and M. Gusman, Pemodelan Dan Perhitungan Volume Akuifer Dengan Menggunakan Metode Indicator Kriging Di Kec. Koto Tangah Dan Kec . Pauh Kota, vol. 5, no. 1, pp. 131–142.
4. L. Octonovrilna and Supriyanto, Velocity modeling of Rayleigh wave in Fault Semangko Padang region using Ambient Noise Tomography method, *AIP Conf. Proc.*, vol. 1729, 2016, https://doi.org/10.1063/1.4946984.
5. P. Razi, J. T. S. Sumantyo, D. Perissin, and Y. Yulkifli, Potential Landslide Detection in Kelok Sembilan Flyover Using SAR Interferometry, *Int. J. Adv. Sci. Eng. Inf. Technol.*, vol. 11, no. 2, pp. 720–728, 2021, https://doi.org/10.18517/ijaseit.11.2.13767.
6. Y. Huang and Z. Wen, Recent developments of soil improvement methods for seismic liquefaction mitigation, *Nat. Hazards*, vol. 76, no. 3, pp. 1927–1938, 2015, https://doi.org/10.1007/s11069-014-1558-9.
7. G. Alexandr, T. N. Chi, and C. Author, Liquefaction Possibility of Soil Layers During, *Int. J. Geomate*, vol. 13, no. 2, pp. 148–155, 2017.
8. S. Lirer and L. Mele, On the apparent viscosity of granular soils during liquefaction tests, *Bull. Earthq. Eng.*, vol. 17, no. 11, pp. 5809–5824, 2019, https://doi.org/10.1007/s10518-019-00706-0.
9. G. Wang and J. Wei, "Microstructure evolution of granular soils in cyclic mobility and post-liquefaction process," *Granul. Matter*, vol. 18, no. 3, 2016, https://doi.org/10.1007/s10035-016-0621-5.
10. J. E. Daniell, A. M. Schaefer, and F. Wenzel, Losses associated with secondary effects in earthquakes, *Front. Built Environ.*, vol. 3, no. June, pp. 1–14, 2017, https://doi.org/10.3389/fbuil.2017.00030.

11. A. Abbaszadeh Shahri, Assessment and Prediction of Liquefaction Potential Using Different Artificial Neural Network Models: A Case Study, *Geotech. Geol. Eng.*, vol. 34, no. 3, pp. 807–815, 2016, https://doi.org/10.1007/s10706-016-0004-z.
12. R. Kamran Disfani and A. Bazrafshan Moghaddam, Identification of soil liquefaction occurrence using wavelet analysis, *SN Appl. Sci.*, vol. 2, no. 10, 2020, https://doi.org/10.1007/s42452-020-03479-3.
13. S. A. Lestari, Pemanfaatan Citra Satelit ALOS-PALSAR untuk Pemetaan Kelembaban Tanah (Studi Kasus: Wilayah Kabupaten Paser, Kalimantan Timur), 2018.
14. S. U. Susha Lekshmi, D. N. Singh, and M. Shojaei Baghini, A critical review of soil moisture measurement, *Meas. J. Int. Meas. Confed.*, vol. 54, pp. 92–105, 2014, https://doi.org/10.1016/j.measurement.2014.04.007.
15. D. D. Alexakis, F. D. K. Mexis, A. E. K. Vozinaki, I. N. Daliakopoulos, and I. K. Tsanis, Soil moisture content estimation based on Sentinel-1 and auxiliary earth observation products. A hydrological approach, *Sensors (Switzerland)*, vol. 17, no. 6, pp. 1–16, 2017, https://doi.org/10.3390/s17061455.
16. J. Peng, A. Loew, S. Zhang, J. Wang, and J. Niesel, Spatial Downscaling of Satellite Soil Moisture Data Using a Vegetation Temperature Condition Index, *IEEE Trans. Geosci. Remote Sens.*, vol. 54, no. 1, pp. 558–566, 2016, https://doi.org/10.1109/TGRS.2015.2462074.
17. Y. Izumi *et al.*, Potential of soil moisture retrieval for tropical peatlands in Indonesia using ALOS-2 L-band full-polarimetric SAR data, *Int. J. Remote Sens.*, vol. 40, no. 15, pp. 5938–5956, 2019, https://doi.org/10.1080/01431161.2019.1584927.
18. L. Renaldi, S. Hadiyoso, D. N. Ramadan, and S. Pd, PROTOTIPE RADAR SEBAGAI PENDETEKSI OBJEK Radar Prototype as Objects Detector, *Appl. Sci.*, vol. 3, no. 3, pp. 2159–2165, 2017.
19. Z. Abidin, D. Fadila, and M. F. E. Purnomo, Analisis Dan Simulasi Parameter Radar Terhadap Performansi Synthetic Aperture Radar Pada Tahap Awal Pencitraan Sensor Radar, *J. Mhs. Teub*, vol. 2, no. 3, pp. 1–7, 2012.
20. P. Razi, J. T. S. Sumantyo, D. Perissin, H. Kuze, M. Y. Chua, and G. F. Panggabean, 3D land mapping and land deformation monitoring using persistent scatterer interferometry (PSI) ALOS PALSAR: Validated by Geodetic GPS and UAV, *IEEE Access*, vol. 6, pp. 12395–12404, 2018, https://doi.org/10.1109/ACCESS.2018.2804899.
21. A. Reigber *et al.*, The high-resolution digital-beamforming airborne SAR system DBFSAR, *Remote Sens.*, vol. 12, no. 11, 2020, https://doi.org/10.3390/rs12111710.
22. F. Octaviany, H. Wijanto, and A. D. Prasetyo, The Comparison of Microstrip Antenna Circle and Square Patch Circularly Polarized for Synthetic Aperture Radar Frequency 1. 27 GHz, vol. 3, no. 3, pp. 1–9, 2016.
23. R. Prastyani and A. Basith, Deteksi Tumpahan Minyak Di Selat Makassar Dengan Penginderaan, *Elipsoida*, vol. 02, no. July, pp. 88–94, 2019.
24. S. Shin, Y. Kim, I. Hwang, J. Kim, and S. Kim, Coupling denoising to detection for SAR imagery, *Appl. Sci.*, vol. 11, no. 12, 2021, https://doi.org/10.3390/app11125569.
25. H. Tanveer, T. Balz, F. Cigna, and D. Tapete, Monitoring 2011–2020 traffic patterns in Wuhan (China) with COSMO-SkyMed SAR, amidst the 7th CISM military world games and COVID-19 outbreak, *Remote Sens.*, vol. 12, no. 10, 2020, https://doi.org/10.3390/rs12101636.
26. B. Septiana, A. Wijaya, and A. Suprayogi, Analisis Perbandingan Hasil Orthorektifikasi Metode Range Doppler Terrain Correction Dan Metode Sar Simulation Terrain Correction Menggunakan Data Sar Sentinel ?? 1, *J. Geod. Undip*, vol. 6, no. 1, pp. 148–157, 2017.
27. D. Kushardono and A. Widipaminto, Kajian Awal Kebutuhan Teknologi Satelit Penginderaan Jauh untuk Mendukung Program REDD di Indonesia, *Maj. Inderaja*, vol. 2, no. 3, pp. 32–38, 2011.
28. I. H. Pradana, L. Y. Irawan, D. Setiawan, F. S. Yuliano, and H. A. Mufid, Analisis Daerah Tergenang Banjir Di Desa Sitiarjo, Kabupaten Malang Menggunakan Data SAR (Synthetic Aperture Radar) Sentinel-1, no. 3, pp. 58–67, 2020.
29. P. Razi *et al.*, 3D modeling using structure from motion technique for land observation in Kelok 9 flyover, *J. Phys. Conf. Ser.*, vol. 1876, no. 1, 2021, https://doi.org/10.1088/1742-6596/1876/1/012026.

30. P. Razi, J. Tetuko, S. Sumantyo, D. Perissin, and A. Munir, Persistent Scattering Interferometry SAR based Velocity and Acceleration Analysis of Land Deformation : Case Study on Kelok Sembilan Bridge, pp. 9–12, 2017.
31. J. Widodo *et al.*, Land subsidence rate analysis of Jakarta Metropolitan Region based on D-InSAR processing of Sentinel data C-Band frequency, *J. Phys. Conf. Ser.*, vol. 1185, no. 1, 2019, https://doi.org/10.1088/1742-6596/1185/1/012004.
32. F. Sarjani, Pengolahan Citra Satelit Alos Palsar Menggunakan Metode Polarimetri Untuk Klasifikasi Lahan Wilayah Kota Padang, vol. 18, no. 1, 2017.
33. P. Razi, J. T. Sri Sumantyo, Yulkifli, J. Widodo, D. Perissin, and Jefriza, Land deformation modeling of Taiwan earthquake using interferometry technique, *J. Phys. Conf. Ser.*, vol. 1481, no. 1, pp. 6–11, 2020, https://doi.org/10.1088/1742-6596/1481/1/012009.
34. R. Sonobe, H. Tani, X. Wang, and M. Fukuda, Estimation of Soil Moisture for Bare Soil Fields Using ALOS/PALSAR HH Polarization Data, *Agric. Inf. Res.*, vol. 17, no. 4, pp. 171–177, 2008, https://doi.org/10.3173/air.17.171.
35. G. C. Topp, J. L. Davis, and A. P. Annan, Electromagnetic determination of soil water content: Measurements in coaxial transmission lines, *Water Resour. Res.*, vol. 16, no. 3, pp. 574–582, 1980, https://doi.org/10.1029/WR016i003p00574.
36. H. Warman and D. Y. Jumas, Kajian Potensi Likuifaksi Pasca Gempa Dalam Rangka Mitigasi Bencana Di Padang, *J. Rekayasa Sipil*, vol. 9, no. 2, p. 1, 2013, https://doi.org/10.25077/jrs.9.2.1-19.2013.